J|A|C|S COMMUNICATIONS

Published on Web 03/03/2010

Metal−Organic Polyhedral Frameworks: High H_2 Adsorption Capacities and Neutron Powder Diffraction Studies

Yong Yan,[†] Irvin Telepeni,[‡] Sihai Yang,[†] Xiang Lin,[†] Winfried Kockelmann,[§] Anne Dailly,[⊥] Alexander J. Blake,[†] William Lewis,[†] Gavin S. Walker,[‡] David R. Allan,[¶] Sarah A. Barnett,[¶] Neil R. Champness,[†] and Martin Schröder*[,†]

School of Chemistry, University of Nottingham, University Park, NG7 2RD, U.K., Energy and Sustainability Research Division, Engineering Faculty, University of Nottingham, University Park, NG7 2RD, U.K., Science and Technology Facilities Council (STFC), Rutherford Appleton Laboratory, ISIS Facility, Didcot, OX11 0QX, U.K., Chemical Sciences and Materials Systems Lab, General Motors LLC, Warren, Michigan 48090, and Diamond Light Source, Harwell Science and Innovation Campus, Didcot, Oxfordshire, OX11 0DE, U.K.

Received January 9, 2010; E-mail: M.Schroder@nottingham.ac.uk

Hydrogen (H_2) is widely considered to be a potential alternative to fossil fuels for mobile applications because of its environmental benefit and high energy density.[1] However, development of an efficient on-board storage system remains a challenge.[2] Porous metal−organic frameworks (MOFs) have been intensively investigated for H_2 storage[3,4] and, compared to other physisorbents such as porous zeolites and carbon materials,[5] have the advantages of high internal surface areas and pore volumes[6] coupled to tunable pore sizes[4] and functional walls.[7] MOFs show significant H_2 uptake by mass, but this is only achieved at low temperatures owing to the weak isosteric heats of adsorption involved (typically 5−8 kJ/mol).[8] Indeed, it has been estimated that an adsorption heat of 15−25 kJ/mol is required for materials operating at 298 K within the pressure range 1.5−20 bar.[9] Various strategies are being pursued for the enhancement of H_2 binding within these metal−organic hybrid materials. These include generating frameworks with narrow pores to allow a single H_2 molecule to interact with the overlapping potential from pore walls,[10] doping with metal ions (Li, Mg),[11] cation exchange to introduce strong electrostatic fields within the cavities,[12] doping with metal nanoparticles to increase H_2 uptake via hydrogen spillover,[13] and incorporation of exposed metal sites.[4,14]

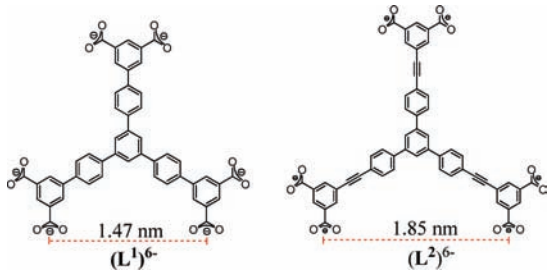

The use of metal−organic polyhedra as building blocks for the construction of porous frameworks is an efficient strategy, since the inherent cavities of the fused polyhedra are maintained on tessellation in space.[15,16] We report herein (i) the synthesis, structure, and gas storage properties of $[Cu_3(L^2)_2]$ (NOTT-116) constructed from the elongated nanosized hexa-carboxylate linker $(L^2)^{6-}$ and (ii) a neutron powder diffraction (NPD) study on fully desolvated $[Cu_3(L^1)_2]$ (NOTT-112)[16] which confirms, for the first time, a unique preferential binding of D_2 within the smallest cuboctahedral cage which incorporates 12 open Cu(II) sites.

Reaction of $Cu(NO_3)_2 \cdot 3H_2O$ with H_6L^2 in DMF/H_2O containing HCl afforded blue crystals of fully solvated NOTT-116, $[Cu_3(C_{54}H_{24}O_{12})(H_2O)_3] \cdot 16DMF \cdot 26H_2O$, which crystallizes in space group $Fm\bar{3}m$ with $a = 51.670(6)$ Å. Three coplanar isophthalate units of the C_3 symmetrical linker $(L^2)^{6-}$ connect to 6 $\{Cu_2(COO)_4\}$ paddlewheels to form a hexagonal face. A cuboctahedral cage (cage A) is thus constructed from 24 isophthalate units and 12 $\{Cu_2(COO)_4\}$ paddlewheels and serves as a 24-connected node to give an overall (3,24)-connected network of **rht**[17] topology. Two other types of cages are generated within NOTT-116: a truncated tetrahedron (cage B) with four triangular windows and four hexagonal faces, and a truncated octahedron (cage C) with six square windows and eight hexagonal faces. These cages A−C have inner sphere diameters of *ca* 1.3, 1.6, and 2.4 nm, respectively.

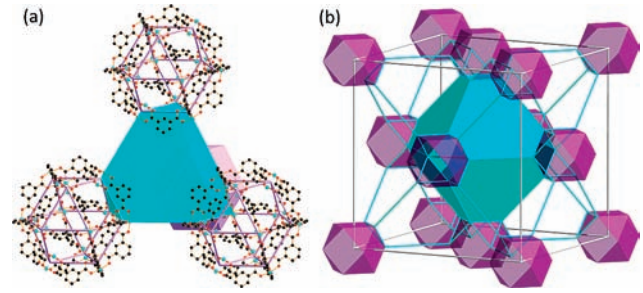

Figure 1. (a) The packing of four cuboctahedra and a truncated tetrahedron; (b) packing of cuboctahedra (in violet) in the framework of NOTT-116 generating a face centered cubic structure. The hexagonal face is shown in turquoise.

The frameworks of NOTT-112 and NOTT-116 have the same **rht** topology and contain the same cuboctahedral cages but differ in their ligand linkers. Both structures can be seen as the face-centered cubic packing of cuboctahedral cages which are connected to form a rigid network (Figure 1). The distance between two adjacent cuboctahedra (expressed as the separation between the centers of the Cu(II) paddlewheels of two closest cuboctahedra) in NOTT-112 is 1.47 nm; this distance increases to 1.85 nm in NOTT-116. Using the PLATON/VOID[18] routine, the total solvent-accessible volume for desolvated NOTT-116 after removal of guest solvates and coordinated water molecules is estimated to be 81%. It should be noted that despite incorporating nanosized linkers and cavities, NOTT-116 is very stable up to 300 °C after the removal of solvent and coordinated water. This high thermal stability for a

[†] School of Chemistry, University of Nottingham.
[‡] Engineering Faculty, University of Nottingham.
[§] Rutherford Appleton Laboratory.
[⊥] General Motors Corporation.
[¶] Diamond Light Source.

10.1021/ja1001407

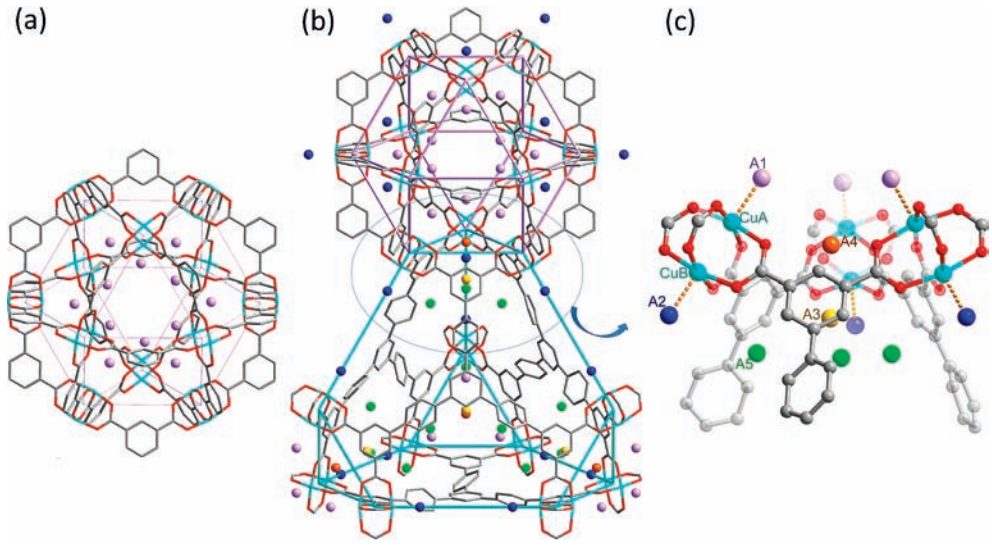

Figure 2. Views of D_2 positions in the desolvated framework of NOTT-112: (a) D_2 positions in the cuboctahedral cage at D_2 loading as 0.5 D_2/Cu; (b) D_2 positions in the cage A and cage B at 2.0 D_2/Cu D_2 loading; (c) view of five D_2 positions (A_1, A_2, A_3, A_4, and A_5) at 2.0 D_2/Cu D_2 loading; gray, carbon; red, oxygen; turquoise, copper. The D_2 positions are represented by colored spheres: A_1, lavender; A_2, blue; A_3, yellow; A_4, orange; A_5, green.

noninterpenetrated and highly porous structure is probably due to the specific arrangements of the stable cuboctahedral cages and the small windows containing Cu(II) paddlewheels and carboxylate units, which connect together to form large cavities.[16,15d]

The permanent porosity of activated NOTT-116 was confirmed by N_2 and Ar adsorption isotherms (see Supporting Information), which show pseudo-type I adsorption behavior. Both sets of isotherms show changes of slope between 0.01 to 0.2 bar, as for NOTT-112, indicating that the different sized cavities are filled in sequence as the pressure increases from below 0.01 to 0.2 bar. The apparent surface area of the desolvated NOTT-116 was estimated using the Brunauer−Emmett−Teller (BET) method to be 4664 m^2/g, comparable to the highest porous MOF and covalent organic framework (COF) materials reported to date.[19] The pore-size distribution calculated from analysis of the Ar isotherm at 87 K using nonlocal density functional theory (NLDFT)[20] confirms distributions around 1.6, 2, and 2.6 nm, consistent with the pore sizes calculated from the crystal structure determination. Significantly, the total pore volume calculated from the Ar sorption isotherm is 2.17 cm^3/g, an ultrahigh pore volume for a porous MOF material.[6b]

High pressure volumetric H_2 sorption isotherms of desolvated NOTT-116 from 0−50 bar at 77 K reveal an excess H_2 uptake reaching 68.4 mg/g, equivalent to 6.4 wt % [wt % = 100(weight of adsorbed H_2)/(weight of host material + weight of adsorbed H_2)] at 27 bar. The total H_2 uptake for NOTT-116 was calculated from the pore volume derived from the Ar sorption isotherm accompanied by H_2 density at different pressures[21] to reach 9.2 wt % at 50 bar. Significantly, the maximum excess H_2 uptake for NOTT-116 is *lower* than that for NOTT-112 (7.07 wt % at 35 bar at 77 K) even though the latter shows a lower internal surface area (3800 m^2/g). This confirms that mesoporous materials with higher internal surface areas and pore volumes do not necessarily guarantee higher H_2 adsorption capacities.[3d,4b,19a] However, NOTT-116 can adsorb a respectable 1.9 wt % of H_2 at 78 K and 1 bar, which is lower than NOTT-112 (2.3 wt %), but still higher than other MOFs without open metal sites. The isosteric heat of adsorption for H_2 calculated by fitting H_2 isotherms at 78 and 88 K using virial-type[22] equations is 6.7 kJ mol^{-1} at zero coverage, greater than other Zn(II)-based porous MOFs and COFs with high H_2 storage capacities.[3b,19a,23]

This low pressure efficiency can be attributed to the high affinity of H_2 molecules to exposed Cu(II) centers and the presence of the relatively small cuboctahedral cage (Figure 1).[16,24,25] This motivated us to investigate the specific positions of adsorbed H_2 within the polyhedral structure, and we, therefore, undertook in situ NPD studies on desolvated NOTT-112 adsorbing D_2 gas at surface coverages of 0.5, 1.0, 1.5, and 2.0 D_2 per Cu (a loading of 1.0 D_2/Cu is equivalent to a H_2 uptake of ∼0.6 wt %). The NPD data were refined combining the Lebail fitting and Rietveld analysis as implemented within GSAS-EXPGUI.[26,27] Following refinement using a starting model derived from the single crystal X-ray structure of NOTT-112,[16] differential nuclear scattering Fourier maps revealed the adsorbed molecular deuterium positions. The refinements for the gas-free and gas-loaded NOTT-112 gave good agreement between the simulated and experimental patterns. No shift of peaks in the diffraction data was observed on D_2 loading suggesting that there is no overall structural change in the framework. At 0.5 D_2 per Cu, two sites were occupied. The first site (site A_1, Figure 2) was found at the exposed Cu(II) ions CuA sited within the cuboctahedral cage with a D_2(centroid)−CuA distance of 2.23 (1) Å suggesting significant interaction between CuA and D_2. The second site A_2 was located on the corresponding CuB site. Interestingly, the refinements at low coverage showed a clear distinction between the D_2 adsorption at the CuA and CuB sites with 85% of the D_2 from the first dosing coordinating to CuA centers, indicating that the two Cu(II) sites exhibit different environments for D_2 binding. Previous NPD studies on HKUST-1[24a] and NOTT-101[4a] in which the Cu(II) centers are chemically equivalent showed no significant differentiation between the Cu sites for D_2 adsorption. Furthermore, for NOTT-112, the $D_2(A_2)$−CuB distance was found to be 2.41 (1) Å (similar to the D_2−Cu distance observed in HKUST-1[24a]), but much longer than $D_2(A_1)$−CuA [2.23 (1) Å]. The preferential adsorption to CuA over CuB is probably due to the former being within the cuboctahedral cage.[25a] At 1.00 D_2 per Cu, there was adsorption at a third site, A_3, accounting for 6% of the adsorbed D_2 and located between three phenyl rings around the 3-fold axis of the triangular window connecting cage A with cage B (Figure 2).[16] At this loading a fourth adsorption site, A_4, was also identified, accounting for 4% of the adsorbed D_2. This site is located on the other side of the triangular

window from A_3, but on the same 3-fold axis. At 1.5 D_2 per Cu, the extra D_2 being added is split between A_2, A_3, and A_4, and a fifth site A_5 starts to be occupied. This latter site is located within the truncated tetrahedral cage B around the 3-fold axis of the triangular window. The total amount of D_2 molecules found from the Rietveld analysis was close to the experimental values for the D_2 loadings. However, for the highest loading, 2.00 D_2 per Cu, the D_2 accounted for is 15% less than that admitted to the sample, which is in part due to non-site-specific adsorption of D_2 through the porous structure.

In conclusion, by incorporating a nanosized C_3 symmetrical ligand within a network of **rht** topology, we have successfully generated noninterpenetrated, mesoporous NOTT-116, which shows a very high BET surface area of 4664 m^2/g, and a total H_2 adsorption capacity of 9.2 wt % at 77 K and 50 bar. However, the maximum excess H_2 capacity for NOTT-116 of 6.4 wt % at 77 K and 27 bar is lower than for NOTT-112, which has a lower BET surface area of 3800 m^2/g but a higher maximum excess H_2 uptake of 7.07 wt % at 77 K.[16] This indicates that simply increasing the available pore volume may not necessarily lead to an increase in gas uptake, suggesting that there is an optimum pore size for H_2 storage.[3d,4b,19a] Significantly, NOTT-116 shows higher H_2 uptake at 1 bar at 77 K than other materials with BET surface areas of more than 4000 m^2/g. This low-pressure efficiency is attributed to the cuboctahedral cages containing exposed Cu(II) sites. This is confirmed by NPD experiments that reveal that the exposed Cu(II) sites within the smallest cuboctahedral cages are the first and strongest binding sites for D_2 in this material giving an overall discrimination between the two types of exposed Cu(II) sites in NOTT-112. Thus, NPD studies provide, for the first time, direct structural evidence demonstrating that a specific geometrical arrangement of exposed Cu(II) sites, in this case within a cuboctahedral cage, strengthens the interactions between D_2 molecules and open metal sites. This study thus guides us toward new design protocols for materials showing high overall H_2 capacities by targeting key surface area and pore metrics and framework topologies.

Acknowledgment. We thank the EPSRC (U.K. Sustainable Hydrogen Energy Consortium, http://www.uk-shec.org.uk/) and the University of Nottingham for funding. M.S. gratefully acknowledges receipt of a Royal Society Wolfson Merit Award and an ERC Advanced Grant. We are grateful to STFC for access to the GEM diffractometer at ISIS for the neutron diffraction experiments, and we thank Diamond Light Source for the award of access to Beamline I19. I.T. and G.S.W. gratefully acknowledge support from the EU-FP6 HYTRAIN RTN project.

Supporting Information Available: Synthetic details and characterization of ligands and complex, X-ray crystallographic information file (CIF), views of crystal structures, PXRD and TGA data, NPD data and analysis, and analyses of N_2, Ar, and H_2 isotherms. This material is available free of charge via the Internet at http://pubs.acs.org.

References

(1) Schlapbach, L.; Zuttel, A. *Nature* **2001**, *414*, 353–358, and references therein.
(2) DOE Office of Energy Efficiency and Renewable Energy Hydrogen, Fuel Cells and Infrastructure Technologies Program Multi-Year Research, Development and Demonstration Plan. http://www.eere.energy.gov/hydrogenandfuelcells/mypp, accessed 2010.
(3) (a) Kaye, S. S.; Dailly, A.; Yaghi, O. M.; Long, J. R. *J. Am. Chem. Soc.* **2007**, *129*, 14176–14177. (b) Furukawa, H.; Miller, M. A.; Yaghi, O. M. *J. Mater. Chem.* **2007**, *17*, 3197–3204. (c) Zhao, X.; Xiao, B.; Fletcher, A. J.; Thomas, K. M.; Bradshaw, D.; Rosseinsky, M. J. *Science* **2004**, *306*, 1012–1015. (d) Latroche, M.; Surblé, S.; Serre, C.; Mellot-Draznieks, C.; Llewellyn, P. L.; Lee, J.-H.; Chang, J.-S.; Jhung, S. H.; Férey, G. *Angew. Chem., Int. Ed.* **2006**, *45*, 8227–8231. (e) Murray, L. J.; Dincă, M.; Long, J. R. *Chem. Soc. Rev.* **2009**, *38*, 1294−1314. (f) Lin, X.; Jia, J.; Hubberstey, P.; Schröder, M.; Champness, N. R. *CrystEngComm* **2007**, *9*, 438–448.
(4) (a) Lin, X.; Telepeni, I.; Blake, A. J.; Dailly, A.; Brown, C. M.; Simmons, J. M.; Zoppi, M.; Walker, G. S.; Thomas, K. T.; Mays, T. J.; Hubberstey, P.; Champness, N. R.; Schröder, M. *J. Am. Chem. Soc.* **2009**, *131*, 2159–2171. (b) Lin, X.; Jia, J.; Zhao, X. B.; Thomas, K. M.; Blake, A. J.; Champness, N. R.; Hubberstey, P.; Schröder, M. *Angew. Chem., Int. Ed.* **2006**, *45*, 7358–7364. (c) Yang, S.; Lin, X.; Dailly, A.; Blake, A. J.; Champness, N. R.; Hubberstey, P.; Schröder, M. *Chem.−Eur. J.* **2009**, *15*, 4829–4835.
(5) (a) Dillon, A. C.; Jones, K. M.; Bekkedahl, T. A.; Kiang, C. H.; Bethune, D. S.; Heben, M. J. *Nature* **1997**, *386*, 377–379. (b) Zhao, X. B.; Xiao, B.; Fletcher, A. J.; Thomas, K. M. *J. Phys. Chem. B* **2005**, *109*, 8880–8888.
(6) (a) Chae, H. K.; Siberio-Pérez, D. Y.; Kim, J.; Go, Y. B.; Eddaoudi, M.; Matzger, A. J.; O'Keeffe, M.; Yaghi, O. M. *Nature* **2004**, *427*, 523–527. (b) Férey, G.; Mellot-Draznieks, C.; Serre, C.; Millange, F.; Dutour, J.; Surblé, S.; Margiolaki, I. *Science* **2005**, *309*, 2040–2042.
(7) (a) Rowsell, J. L. C.; Millward, A. R.; Park, K. S.; Yaghi, O. M. *J. Am. Chem. Soc.* **2004**, *126*, 5666–5667. (b) Furukawa, H.; Kim, J.; Ockwig, N. W.; O'Keeffe, M.; Yaghi, O. M. *J. Am. Chem. Soc.* **2008**, *130*, 11650–11661. (c) Wu, S.; Ma, L.; Long, L.-S.; Zheng, L.-S.; Lin, W. *Inorg. Chem.* **2009**, *48*, 2436–2442. (d) Yang, W.; Lin, X.; Jia, J.; Blake, A. J.; Wilson, C.; Hubberstey, P.; Champness, N. R.; Schröder, M. *Chem. Commun.* **2008**, 359–361. (e) Tanabe, K. K.; Cohen, S. M. *Angew. Chem., Int. Ed.* **2009**, *48*, 7424–7427. (f) Wang, Z. Q.; Cohen, S. M. *Chem. Soc. Rev.* **2009**, *38*, 1315–1329.
(8) (a) Dincă, M.; Han, W. S.; Liu, Y.; Dailly, A.; Brown, C. M.; Long, J. R. *Angew. Chem., Int. Ed.* **2007**, *46*, 1419–1422. (b) Liu, Y.; Kabbour, H.; Brown, C. M.; Neumann, D. A.; Ahn, C. C. *Langmuir* **2008**, *24*, 4772–4777.
(9) Bhatia, S. K.; Myers, A. L. *Langmuir* **2006**, *22*, 1688–1700.
(10) Belof, J. L.; Stern, A. C.; Eddaoudi, M.; Space, B. *J. Am. Chem. Soc.* **2007**, *129*, 15202–15210.
(11) (a) Himsl, D.; Wallacher, D.; Hartmann, M. *Angew. Chem., Int. Ed.* **2009**, *48*, 4639–4642. (b) Mulfort, K. L.; Farha, O. K.; Stern, C. L.; Sarjeant, A. A.; Hupp, J. T. *J. Am. Chem. Soc.* **2009**, *131*, 3866–3868.
(12) (a) Nouar, F.; Eckert, J.; Eubank, J. F.; Forster, P.; Eddaoudi, M. *J. Am. Chem. Soc.* **2009**, *131*, 2864–2870. (b) Dincă, M.; Long, J. R. *J. Am. Chem. Soc.* **2007**, *129*, 11172–11176. (c) Yang, S.; Lin, X.; Blake, A. J.; Walker, G.; Hubberstey, P.; Champness, N. R.; Schröder, M. *Nature Chem.* **2009**, *1*, 487–493. (d) Yang, S.; Lin, X.; Blake, A. J.; Thomas, K. M.; Hubberstey, P.; Champness, N. R.; Schröder, M. *Chem. Commun.* **2008**, 6108–6110.
(13) (a) Li, Y.; Yang, R. T. *J. Am. Chem. Soc.* **2006**, *128*, 726–727. (b) Tsao, C.-S.; Yu, M.-S.; Wang, C.-Y.; Liao, P.-Y.; Chen, H.-L.; Jeng, U.-S.; Tzeng, Y.-R.; Chung, T.-Y.; Wu, H.-C. *J. Am. Chem. Soc.* **2009**, *131*, 1404–1406.
(14) Dincă, M.; Long, J. R. *Angew. Chem., Int. Ed.* **2008**, *47*, 6766–6779.
(15) (a) Perry IV, J. J.; Perman, J. A.; Michael, J.; Zaworotko, M. J. *Chem. Soc. Rev.* **2009**, *38*, 1400–1417, and references therein. (b) Prakash, M. J.; Lah, M. S. *Chem. Commun.* **2009**, 3326–3341. (c) Nouar, F.; Eubank, J. F.; Bousquet, T.; Wojtas, L.; Zaworotko, M. J.; Eddaoudi, M. *J. Am. Chem. Soc.* **2008**, *130*, 1833–1835. (d) Zhao, D.; Yuan, D.; Sun, D.; Zhou, H.-C. *J. Am. Chem. Soc.* **2009**, *131*, 9186–9188.
(16) Yan, Y.; Lin, X.; Yang, S.; Blake, A. J.; Dailly, A.; Champness, N. R.; Hubberstey, P.; Schröder, M. *Chem. Commun.* **2009**, 1025–1027.
(17) Delgado-Friedrichs, O.; O'Keeffe, M. *Acta Crystallogr.* **2007**, *A63*, 344–347.
(18) Spek, A. L. *PLATON. Acta Crystallogr., Sect. D* **2009**, *65*, 148–155.
(19) (a) Koh, K.; Wong-Foy, A. G.; Matzger, A. J. *J. Am. Chem. Soc.* **2009**, *131*, 4184–4185. (b) Ben, T.; Ren, H.; Ma, S.; Cao, D.; Lan, J.; Jing, X.; Wang, W.; Xu, J.; Deng, F.; Simmons, J. M.; Qiu, S.; Zhu, G. *Angew. Chem., Int. Ed.* **2009**, *48*, 9457–9460.
(20) Ravikovitch, P. I.; Wei, D.; Chueh, W. T.; Haller, G. L.; Neimark, A. V. *J. Phys. Chem. B* **1997**, *101*, 3671–3679.
(21) H_2 density at 0−50 bar, 77 K from the National Institute of Standards and Technology (NIST) USA. http://webbook.nist.gov/chemistry/fluid/, accessed 2010.
(22) Czepirski, L.; Jagiełło, J. *Chem. Eng. Sci.* **1989**, *44*, 797–801.
(23) Furukawa, H.; Yaghi, O. M. *J. Am. Chem. Soc.* **2009**, *131*, 8875–8883.
(24) (a) Peterson, V. K.; Liu, Y.; Brown, C. M.; Kepert, C. J. *J. Am. Chem. Soc.* **2006**, *128*, 15578–15579. (b) Liu, Y.; Brown, C. M.; Neumann, D. A.; Peterson, V. K.; Kepert, C. J. *J. Alloys Compd.* **2007**, *446*, 385–388.
(25) (a) Wang, X.-S.; Ma, S.; Forster, P. M.; Yuan, D.; Eckert, J.; López, J. J.; Murphy, B. J.; Parise, J. B.; Zhou, H.-C. *Angew. Chem., Int. Ed.* **2008**, *47*, 7263–7266. (b) Hong, S.; Oh, M.; Park, M.; Yoon, J. W.; Chang, J.-S.; Lah, M. S. *Chem. Commun.* **2009**, 5397–5399.
(26) Larson, A. C.; Dreele, R. B. V. *General Structure Analysis System (GSAS)*; LAUR Report; Los Alamos National Laboratory: Los Alamos, NM, 2000; pp 86−748.
(27) Toby, B. H. *J. Appl. Crystallogr.* **2001**, *34*, 210–213.

JA1001407